

## *Supporting Information*

# Growth of 2H Stacked WSe<sub>2</sub> Bilayers on Sapphire

*Ali Han<sup>1</sup>, Areej Aljarb<sup>1</sup>, Sheng Liu<sup>2</sup>, Peng Li<sup>1</sup>, Chun Ma<sup>1</sup>, Fei Xue<sup>1</sup>, Sergei Lopatin<sup>3</sup>, Chih-Wen Yang<sup>1</sup>, Jing-Kai Huang,<sup>1,4</sup> Yi Wan<sup>1</sup>, Xixiang Zhang<sup>1</sup>, Kuo-Wei Huang<sup>1</sup>, Qihua Xiong<sup>5</sup>, Vincent Tung<sup>1,6\*</sup>, Thomas D. Anthopoulos<sup>1\*</sup>, Lain-Jong Li<sup>1,4\*</sup>*

<sup>1</sup>Physical Sciences and Engineering Division (PSE), King Abdullah University of Science and Technology, Thuwal 23955-6900, Kingdom of Saudi Arabia

<sup>2</sup>Division of Physics and Applied Physics, School of Physical and Mathematical Sciences, Nanyang Technological University, Singapore 637371

<sup>3</sup>King Abdullah University of Science and Technology (KAUST), Core Labs, Thuwal, 23955-6900, Kingdom of Saudi Arabia

<sup>4</sup>School of Materials Science and Engineering, University of New South Wales, Sydney, NSW 2052, Australia.

<sup>5</sup>Division of Physics and Applied Physics, School of Physical and Mathematical Sciences, Nanyang Technological University, Singapore 637371. MajuLab, CNRS-UNS-NUS-NTU International Joint Research Unit, UMI 3654, Singapore 639798. NOVITAS, Nanoelectronics Center of Excellence, School of Electrical and Electronic Engineering, Nanyang Technological University, Singapore 639798

<sup>6</sup>Molecular Foundry Division, Lawrence Berkeley National Lab, Berkeley 94720, USA

\* E-mails: [thomas.anthopoulos@kaust.edu.sa](mailto:thomas.anthopoulos@kaust.edu.sa); [vincent.tung@kaust.edu.sa](mailto:vincent.tung@kaust.edu.sa); [lance.li@kaust.edu.sa](mailto:lance.li@kaust.edu.sa);

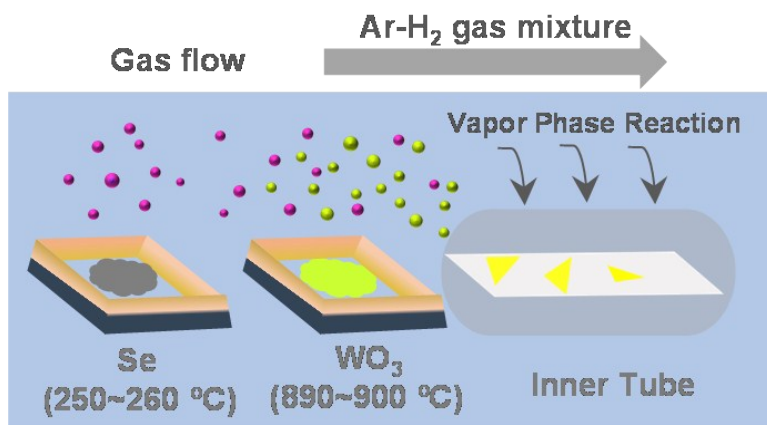


**Figure S1.** Schematic illustration of the CVD setup and the relative position between WO<sub>3</sub>, Se and substrate. The distance between Se powder and WO<sub>3</sub> powder is ~25 cm.

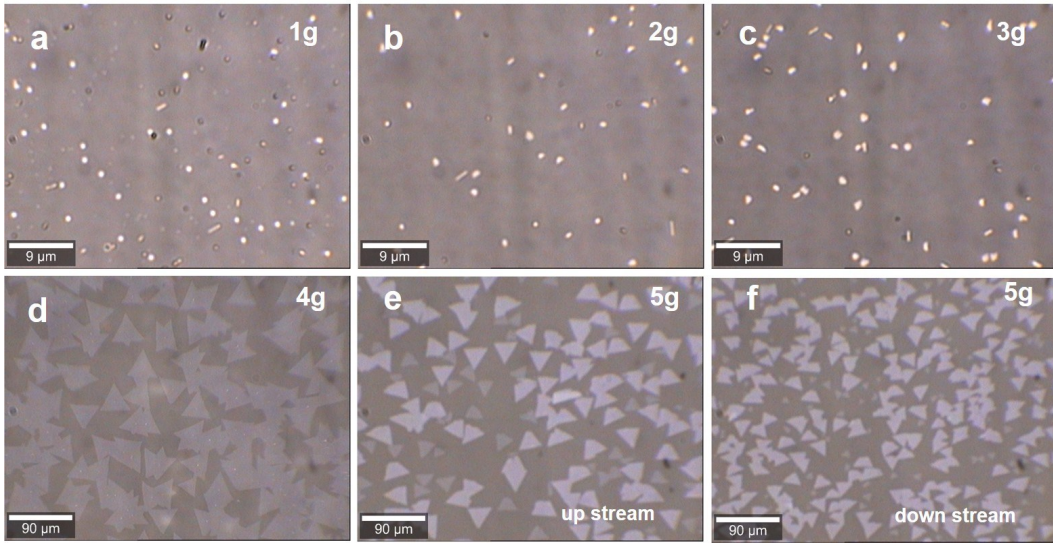


**Figure S2. Optical images for the WSe<sub>2</sub> growth by CVD method.** The mass amount of WO<sub>3</sub> is 0.3g, while the amount of Se powder is increased. The high-purity of H<sub>2</sub>/Ar is as the carrier gas with a fixed flow rate of 5/65 sccm/sccm. The T<sub>Se</sub> (temperature of Se) is maintained at 250 °C while T<sub>WO<sub>3</sub></sub> (the temperature of WO<sub>3</sub>) is kept at 895 °C. The growth pressure of the furnace is 10 torr for the whole CVD growth. The growth time is 15 mins.

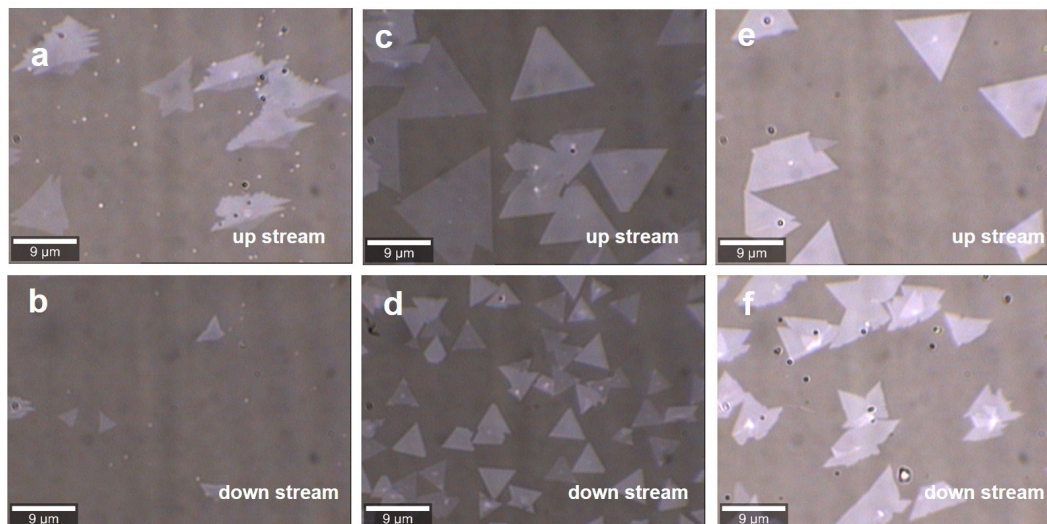


**Figure S3. Optical images for the WSe<sub>2</sub> growth by CVD method.** The mass amount of WO<sub>3</sub> is 0.3 g. The high-purity of H<sub>2</sub>/Ar is as the carrier gas with a fixed flow rate of 5/65 sccm/sccm. **a-b**, The amount of Se powder is 5.5 g, T<sub>Se</sub> = 250 °C and T<sub>WO<sub>3</sub></sub> = 890 °C; **c-d**, The amount of Se powder is 5.0 g, T<sub>Se</sub> = 260 °C and T<sub>WO<sub>3</sub></sub> = 895 °C; **e-f**, The amount of Se powder is 5.5 g, T<sub>Se</sub> = 250 °C and T<sub>WO<sub>3</sub></sub> = 900 °C.

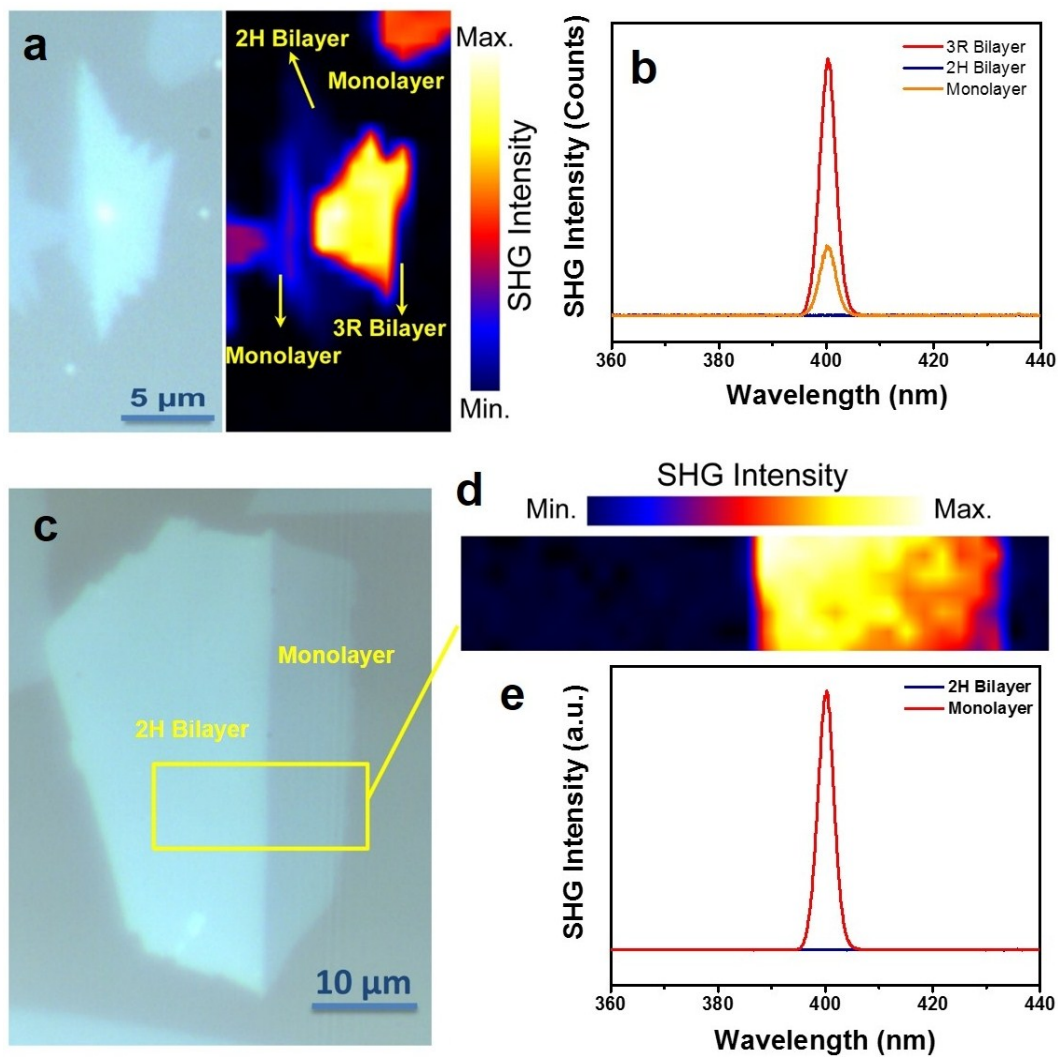


**Figure S4.** **a**, Left: optical micrograph of cloud bilayer WSe<sub>2</sub> crystal with monolayer WSe<sub>2</sub> as reference; Right: The corresponding SHG mapping intensity obtained by pixel-to-pixel spatial scanning on the crystals in Fig. S4a; **b**, The SH signal spectra of different layer number; **c**, Optical micrograph of irregular bilayer WSe<sub>2</sub> crystal with monolayer WSe<sub>2</sub> as reference; **d**, The corresponding SHG mapping intensity obtained by pixel-to-pixel spatial scanning on the crystals in Fig. S4c; **e**, The SH signal spectra of different layer number.

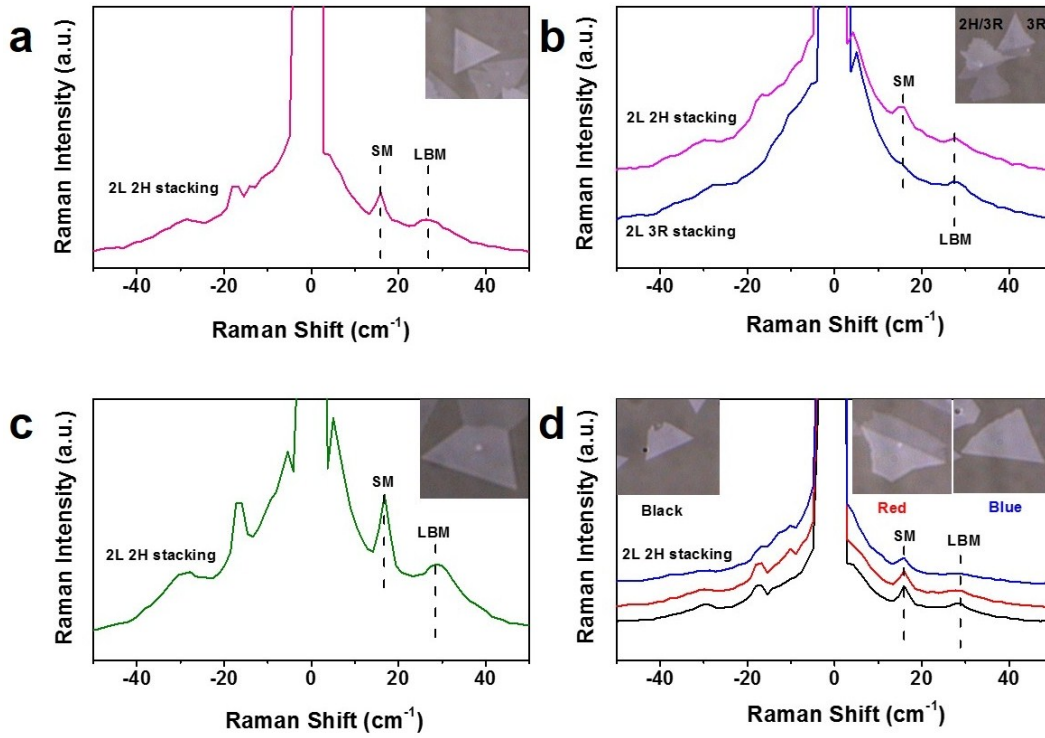


**Figure S5.** Low-frequency Raman spectra of bilayer  $\text{WSe}_2$  crystals for 2H and 3R stacking configurations with different morphologies.

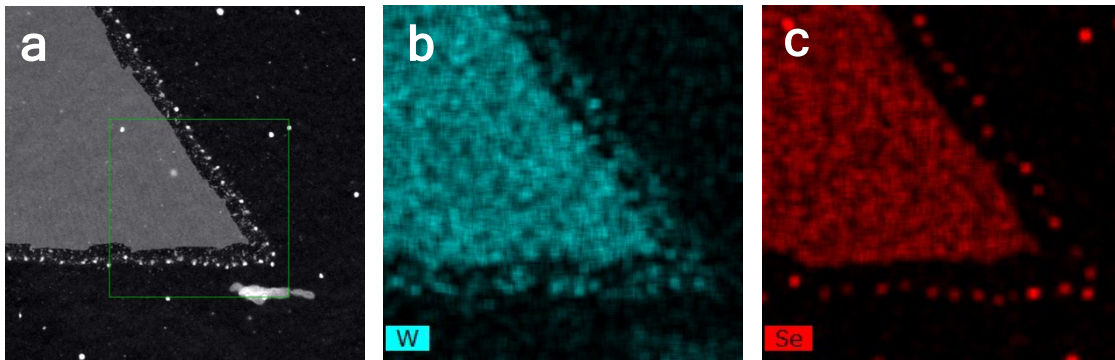


**Figure S6** **a**, Low-magnification HAADF-STEM image of top-view bilayer  $\text{WSe}_2$  sample; **b-c**, elemental mapping of the region (green frame) in Fig.a.



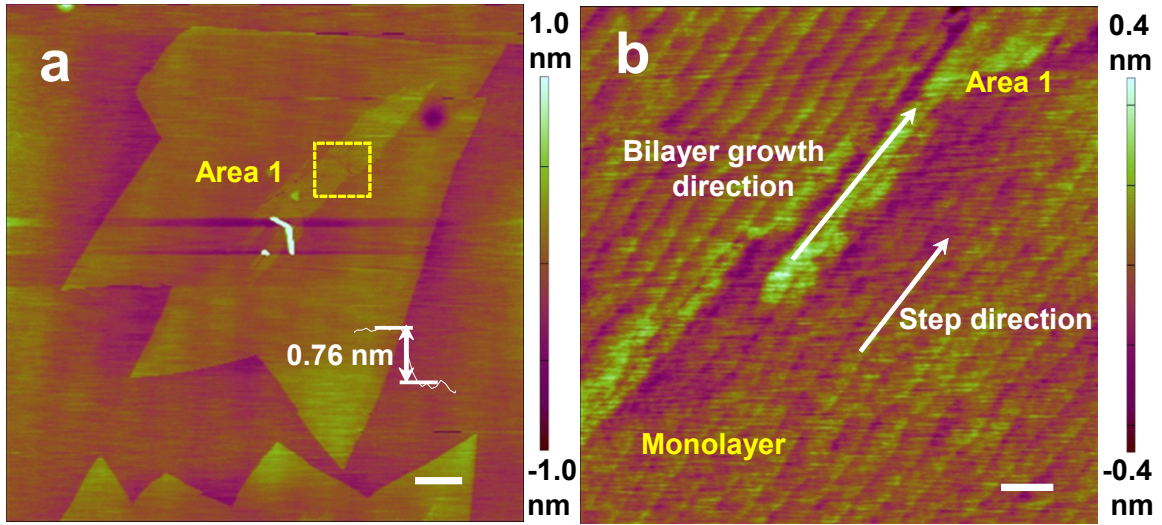


**Figure S7. a**, AFM topographic image of the monolayer WSe<sub>2</sub> grain boundary crystal with bilayer nuclei in the center area; **b**, The zoom-in AFM topographic image of area 1, indicative of initial WSe<sub>2</sub> bilayer nuclei aligned growth on the atomic steps. Scale bars: a, 2  $\mu\text{m}$ ; b, 100 nm.



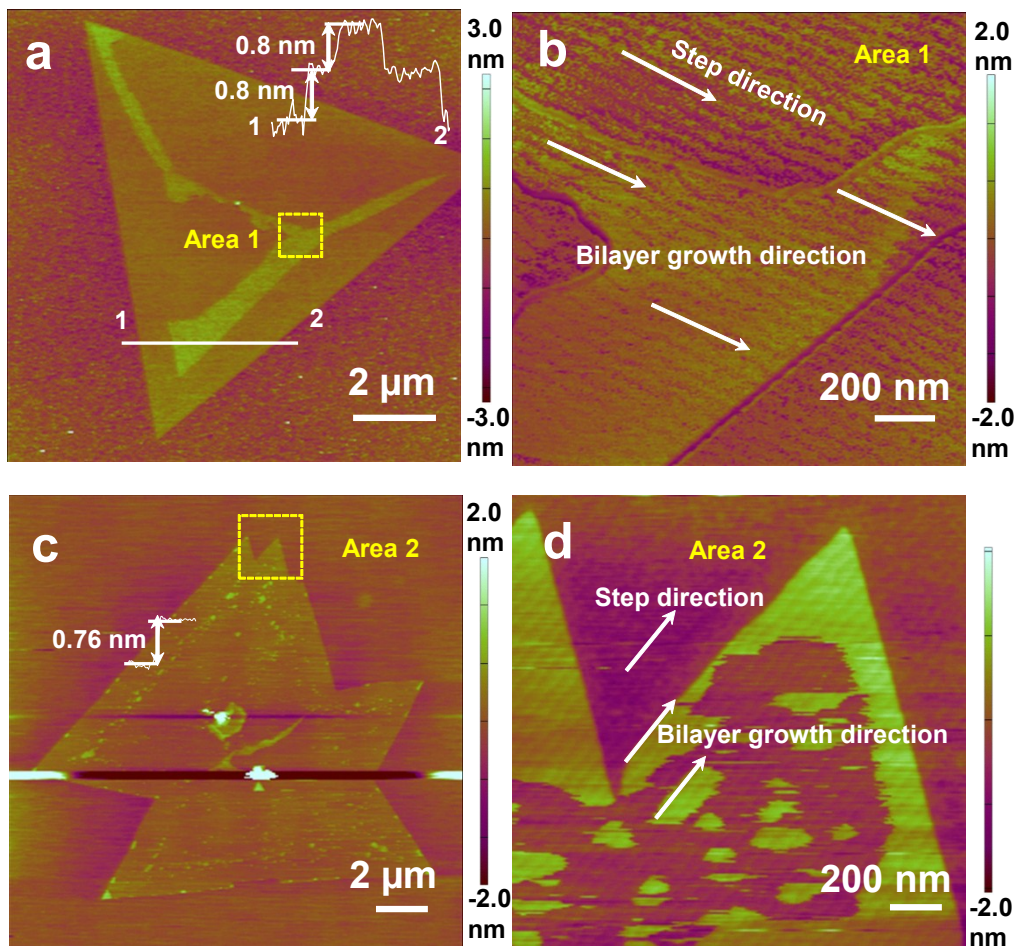


**Figure S8.** **a-b**, AFM topographic images of monolayer WSe<sub>2</sub> crystal with bilayer nuclei in different areas. The inset height profile is ~0.8 nm, indicating a thickness of WSe<sub>2</sub> monolayer. The zoom-in AFM image in Fig. R1b shows WSe<sub>2</sub> bilayer nuclei initial growth on the atomic steps of sapphire; **c-d**, AFM topographic images of monolayer WSe<sub>2</sub> crystal with bilayer nuclei in different areas. The inset height profile is ~0.76 nm, indicating a thickness of WSe<sub>2</sub> monolayer. The zoom-in AFM image in Fig. R1d shows WSe<sub>2</sub> bilayer nuclei initial growth on the atomic steps of sapphire.

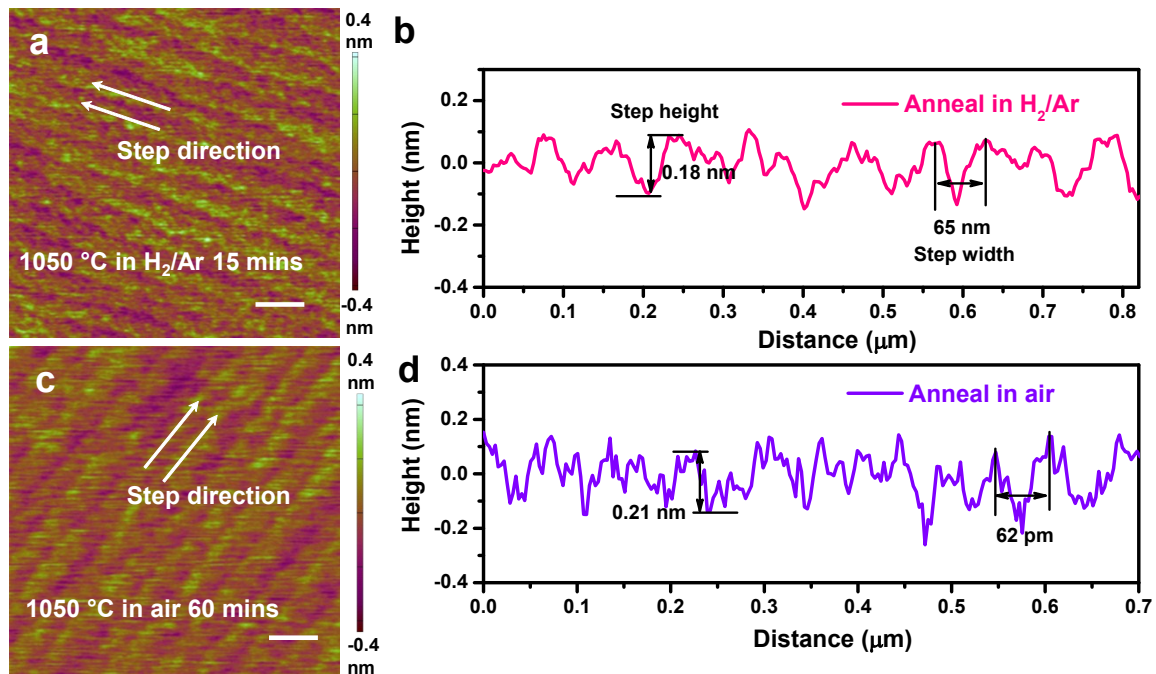


**Figure S9.** **a**, AFM topographic image of sapphire surface after high-temperature treatment (1050 °C in H<sub>2</sub>/Ar for 15 mins); **b**, the corresponding cross-section height profile of the atomic steps along the vertical step direction in Fig. S7a; **c**, AFM topographic image of sapphire surface after high-temperature treatment (1050 °C in air for 60 mins); **d**, the corresponding cross-section height profile of the atomic steps along the vertical step direction in Fig. S7c. Scale bars: a, 100 nm; c, 100 nm.

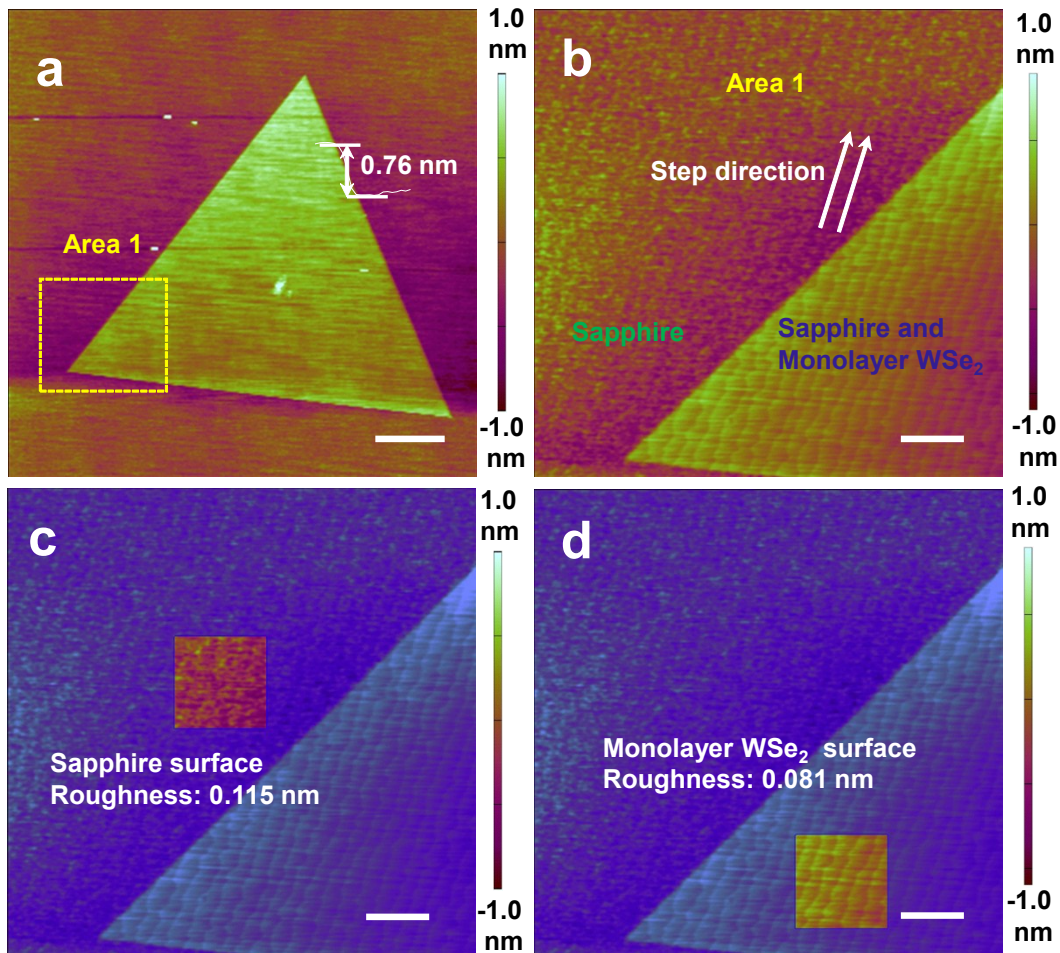


**Figure S10.** **a**, AFM topographic image of one WSe<sub>2</sub> crystal. The inset height profile was  $\sim 0.8$  nm, indicating a monolayer thickness; **b**, The zoom-in AFM image in Fig. S8a. And the image showed irregular atomic steps on bare sapphire surface without any pre-treatment. In contrast, the apparently periodic atomic steps were shown after covering monolayer WSe<sub>2</sub>; **c**, The selected area for the roughness calculation of bare sapphire surface (300 nm x 300 nm); **d**, The selected area for the average roughness calculation of sapphire surface with monolayer WSe<sub>2</sub> covering (300 nm x 300 nm). Scale bars: a, 2  $\mu\text{m}$ ; b, 200 nm; c, 2  $\mu\text{m}$ ; d, 200 nm.

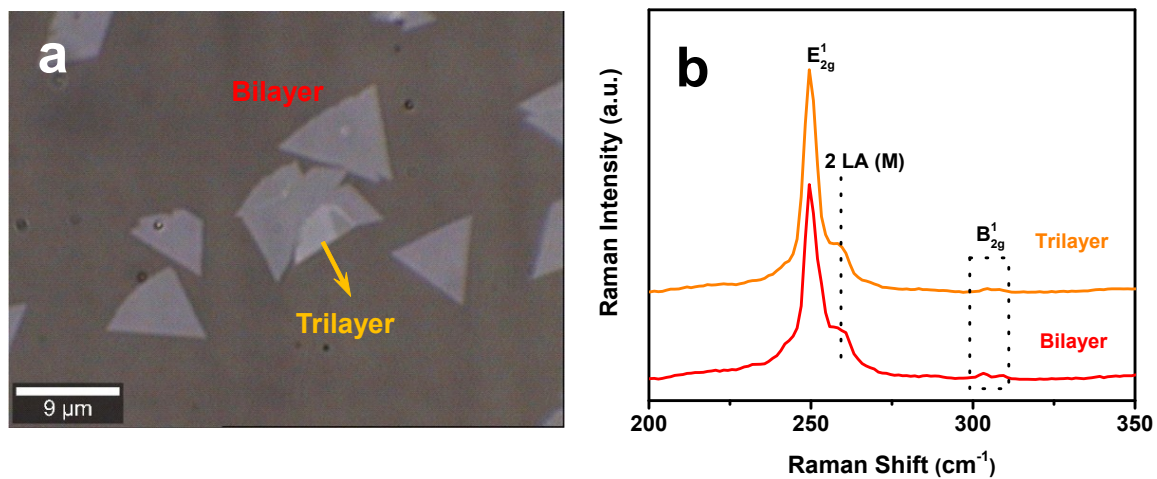


**Figure S11. a**, Optical micrograph of bilayer/trilayer WSe<sub>2</sub> crystals as-grown on c-plane sapphire substrate; **b**, The Raman spectra measurements for bilayer (red) and trilayer (orange) WSe<sub>2</sub> crystals.

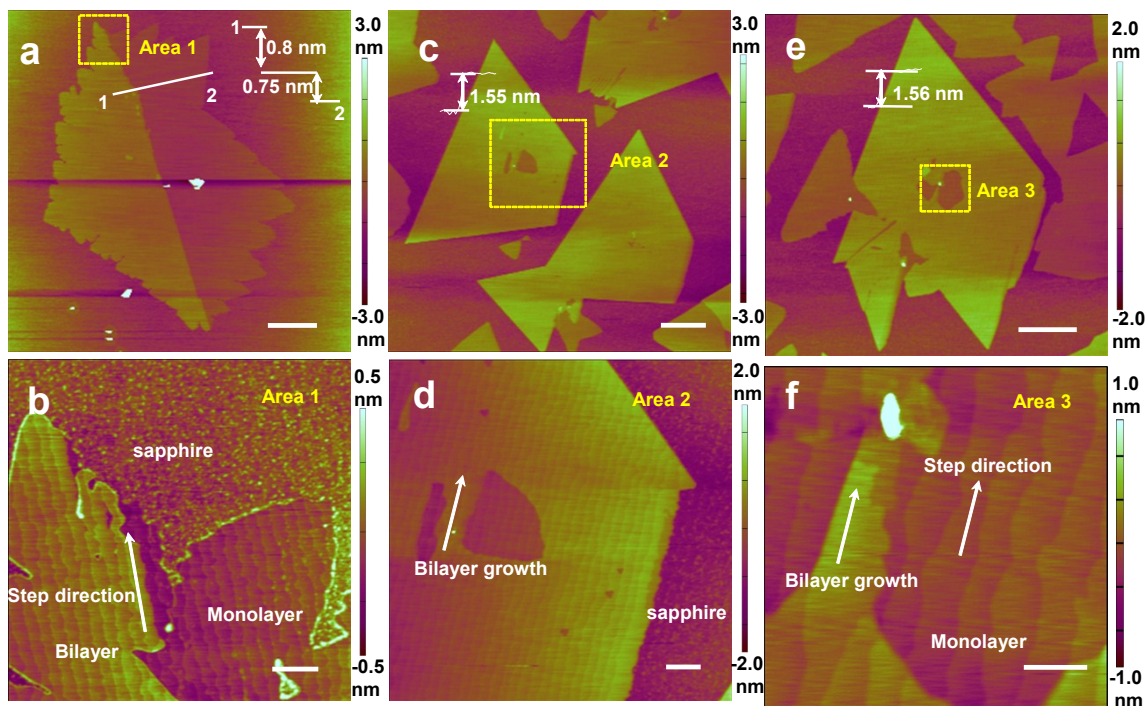


**Figure S12. AFM topographic images of three representative bilayer WSe<sub>2</sub> crystals as-grown on sapphire surface.** **a**, The bilayer WSe<sub>2</sub> crystal with irregular morphology. The inset height profiles were both  $\sim 0.8$  nm, indicating a bilayer thickness in the left part and a monolayer thickness in the right part of the WSe<sub>2</sub> crystal; **b**, The zoom-in AFM image showed the bilayer WSe<sub>2</sub> nuclei growth orientation following the atomic steps; **c**, the bilayer WSe<sub>2</sub> crystal with truncated triangle morphology. The inset height profile demonstrated a bilayer thickness of WSe<sub>2</sub> crystal; **d**, The zoom-in AFM image showed bilayer WSe<sub>2</sub> nuclei growth orientation following the atomic steps; **e**, The bilayer WSe<sub>2</sub> crystal with grain boundary. The inset height profile demonstrated a bilayer thickness of WSe<sub>2</sub>; **f**, The zoom-in AFM image showed bilayer WSe<sub>2</sub> nuclei growth orientation following the atomic steps. Scale bars: a, 2  $\mu$ m; b, 200 nm; c, 1  $\mu$ m; d, 200 nm; e, 1  $\mu$ m; f, 100 nm.

**Table S1. Roughness measurements on different surfaces**

<b>WSe<sub>2</sub> crystals</b>	<b>Sapphire Roughness</b>	<b>Monolayer Roughness</b>	<b>Bilayer Roughness</b>	<b>Trilayer Roughness</b>	<b>Sapphire Roughness (1050 °C)<sup>1</sup></b>	<b>Sapphire Roughness (1050 °C)<sup>2</sup></b>
Sapphire (Fig. S7a)	-	-	-	-	0.056 nm	-
Sapphire (Fig. S7c)	-	-	-	-	-	0.060 nm
Crystal 1 (Fig. 2b)	-	0.070 nm	-	-	-	-
Crystal 2 (Fig. 2d)	0.109 nm	0.073 nm	0.068 nm	-	-	-
Crystal 3 (Fig. 3b)	0.129 nm	0.094 nm	0.097 nm	0.076 nm	-	-
Crystal 4 (Fig. S8b)	0.148 nm	0.056 nm	-	-	-	-
Crystal 5 (Fig. S10b)	0.110 nm	0.077 nm	0.082 nm	-	-	-
Crystal 6 (Fig. S10d)	0.125 nm	0.081 nm	0.073 nm	-	-	-
Crystal 7 (Fig. S10f)	-	0.075 nm	0.086 nm	-	-	-

<sup>1</sup>The as-supplied sapphire was annealed in the H<sub>2</sub>/Ar for 15 mins;

<sup>2</sup>The as-supplied sapphire was annealed in the air for 60 mins.

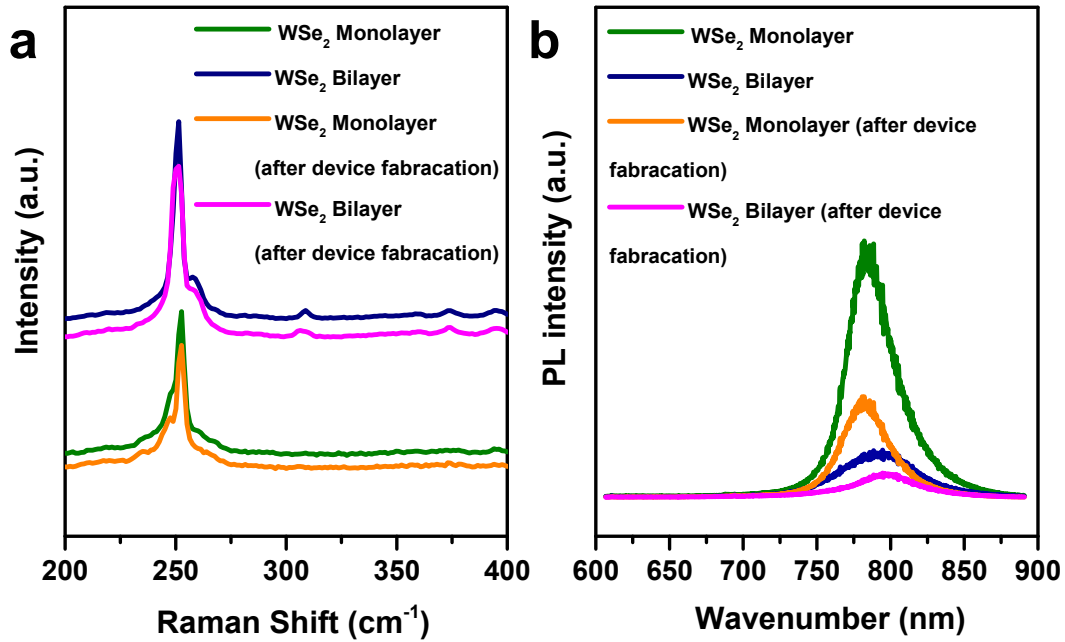


**Figure S13. a.** The Raman spectra measurements for WSe<sub>2</sub> monolayer and bilayer crystals before and after device fabrication on c-plane sapphire substrate; **b,** The PL spectra measurements for WSe<sub>2</sub> monolayer and bilayer crystals before and after device fabrication on c-plane sapphire substrate.

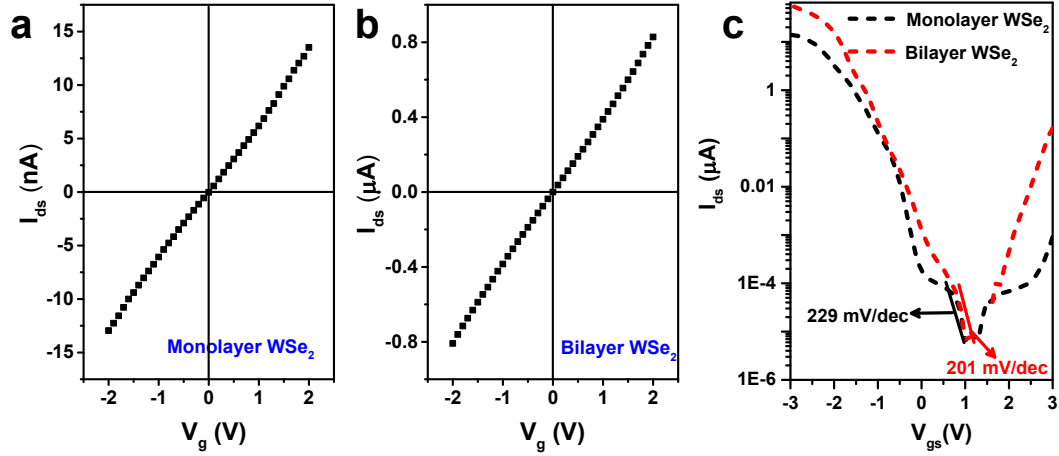


**Figure S14.** **a**,  $I_{ds}$  as a function of  $V_g$  for monolayer device with two terminal.  $I_{ds}$  as a function of  $V_g$  for bilayer device with two terminal; **b**,  $I_{ds}$  as a function of  $V_g$  for monolayer device.  $I_{ds}$  as a function of  $V_g$  for bilayer device.  $C_g = 5.0 \mu\text{F}/\text{cm}^2$ ; **c**,  $I_{ds}$  as a function of  $V_{gs}$  for monolayer/bilayer device. The subthreshold slopes of monolayer and bilayer crystals were measured to be 229 and 201 mV/dec, respectively.